High-Energy Factorization for Drell-Yan process in hadron collisions with new Unintegrated PDFs

M. A. Nefedov[1], and V. A. Saleev[1,2]

[1] Samara National Research University
[2] Joint Institute for Nuclear Research

10.12.2020
Resummation, Evolution, Factorization 2020, Higgs Centre, Edinburgh

Talk is based on: PHYSICAL REVIEW D 102, 114018 (2020); 2009.13188 [hep-ph]

Outline

Introduction

Motivation for theorists

The transverse-momentum ($\mathbf{q}_T$) distribution of Drell-Yan(DY) lepton pairs with large invariant mass $Q \gg \Lambda_{\mathrm{QCD}}$, produced in hadronic collisions, continues to attract a lot of attention from experimentalists:

- High-precision data on the $|\mathbf{q}_T|$-spectrum of lepton pairs with Q close to the Z-boson mass from ATLAS Collaboration at $\sqrt{S} = 13$ TeV
- Data for lower values of Q had been recently published by PHENIX Collaboration at RHIC Collider with $\sqrt{S} = 200$ GeV
- Data obtained at Tevatron by CDF Collaboration at $\sqrt{S} = 1.8$ TeV
- Low-energy ($\sqrt{S} \sim 20 - 30$ GeV) fixed-target experiments in 1980s and early 1990s in CERN and Fermilab (E-288,R-209,E-605)

Introduction

From the theory side

The description of Drell-Yan $|\mathbf{q}_T|$-spectrum at $|\mathbf{q}_T| \ll Q$ have recently reached maturity, with the achievement of Next^3-to-Leading Logarithmic (N^{3}LL) accuracy of the resummation of higher-order perturbative QCD corrections, enhanced by large $\ln \mathbf{q}_T^2/Q^2$, in the context of the Transverse-Momentum Dependent(TMD)-factorization formalism, see:

- I. Scimemi and A. Vladimirov, J. High Energy Phys. 06 811 (2020) 137. 812
- A. Bacchetta, V. Bertone, C. Bissolotti, G. Bozzi, F. Delcarro, F. Piacenza, and M. Radici, J. High Energy Phys. 814 07 (2020) 117.

Introduction

At the same time

It has been observed [A. Bacchetta, G. Bozzi, M. Lambertsen, F. Piacenza, J. Steiglechner, and W. Vogelsang, Phys. Rev. D 100, 014018 819 (2019).], that Next-to-Leading Order calculation of the $|\mathbf{q}_T|$-spectrum in the *Collinear Parton Model(CPM)* of QCD can not describe normalization and shape of low-energy Drell-Yan data in the region $|\mathbf{q}_T| \gtrsim Q$, where $\ln \mathbf{q}_T^2/Q^2$-enhancement of higher-order corrections is not presented and fixed-order predictions should be applicable.

Introduction

A. Bacchetta, et al. *Phys. Rev. D 100, 014018 819 (2019)*

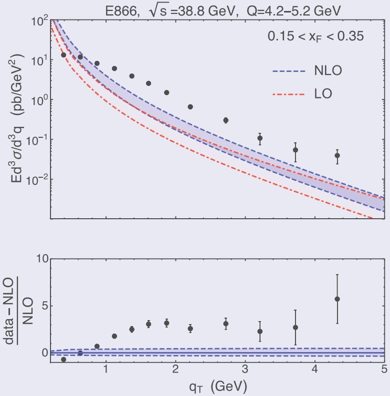

Introduction

In our opinion

- This phenomenological puzzle is a manifestation of deeper theoretical issue with current formulation of TMD-factorization, which does not provide a unique prescription for the matching between TMD (the so-called W-term) and Collinear-factorization (the Y-term) parts of the calculation at $|\mathbf{q}_T| \simeq Q$.
- There is no even QED gauge-invariant definition for the W-term at $|\mathbf{q}_T| \sim Q$,

In the present paper,

we approach the problem of uniform description of the $|\mathbf{q}_T|$-spectrum of Drell-Yan lepton pairs from a point of view of *High-Energy Factorization (HEF)*. Our *Parton Reggeization Approach (PRA)* is a version of HEF, based on the *Modified Multi-Regge Kinematics (MMRK)* approximation for QCD scattering amplitudes. **This approximation is accurate both in the Collinear limit, which drives the TMD-factorization and in the High-Energy (Multi-Regge) limit.**

Parton Reggeization Approach

MRK factorization, $z_{1,2} << 1$ and $\tilde{q}_2^+ << \tilde{q}_2^-$, $\tilde{q}_1^-$ $<< \tilde{q}_1^+$, $\mathbf{q}_T^2/Q^2$ can be arbitrary, $Q^2, Q_T^2 << S$

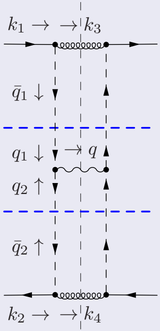

Figure: Diagrammatic representations of squared (M)MRK amplitudes for $q + \bar{q} \rightarrow \gamma^* + 2g$ process . The "small" light-cone momentum components $\bar{q}_1^-$ and $\bar{q}_2^+$ are neglected beyond blue dashed lines. Solid dots denote Fadin-Sherman vertices.

MMRK factorization, from $2 \rightarrow 3$ to $2 \rightarrow 1$ with Reggeized off-shell quarks

We consider auxiliary hard CPM subprocesses:

$$q + \bar{q} \rightarrow \gamma^* + g + g \Rrightarrow Q + \bar{Q} \rightarrow \gamma^*$$

$$g + g \rightarrow \gamma^* + q + \bar{q} \Rrightarrow Q + \bar{Q} \rightarrow \gamma^*$$

$$q + g \rightarrow \gamma^* + q + g \Rrightarrow Q + \bar{Q} \rightarrow \gamma^*$$

$$\Gamma_\mu^{(+-)}(q_1, q_2) = \gamma_\mu - \hat{q}_1 \frac{n_\mu^-}{q_2^-} - \hat{q}_2 \frac{n_\mu^+}{q_1^+} \quad (1)$$

The Fadin-Sherman vertices [V. S. Fadin and V. E. Sherman, JETP Lett. 23, 599 (1976)] which we have applied to the case of Drell-Yan process for the first time in [M. Nefedov, N. Nikolaev, and V. Saleev, Phys. Rev. D 87, 876 014022 (2013)]

LO MMRK factorization formula

See [A. V. Karpishkov, M. A. Nefedov, V. A. Saleev, Phys.Rev. **D96** 096019 (2017)]; M.A. Nefedov, V.A. Saleev, Phys. Rev. **102**, 114018 (2020) for details.

Auxiliary hard CPM subprocess:

$$q(k_1) + \bar{q}(k_2) \to g(k_3) + \gamma^*(q) + g(k_4),$$

where $k_1^2 = 0$, $k_1^- = 0$, $k_2^2 = 0$, $k_2^+ = 0$.
Kinematic variables ($0 < z_{1,2} < 1$):

$$z_1 = \frac{k_1^+ - k_3^+}{k_1^+}, \quad z_2 = \frac{k_2^- - k_4^-}{k_2^-},$$

Two limits where $\overline{|\mathcal{M}|^2}$ factorizes:

1. **Collinear limit:** $\mathbf{k}_{T3,4}^2, \mathbf{q}_T^2 \ll Q^2$, $z_{1,2}$ – arbitrary,
2. **Multi-Regge limit:** $z_{1,2} \ll 1$, $\mathbf{k}_{T3,4}^2$, $\mathbf{q}_T^2$ – arbitrary.

LO MMRK factorization formula

Multi-Regge limit: $z_{1,2} \ll 1$, $\mathbf{k}_{T3,4}^2$ – arbitrary:

$$\overline{|\mathcal{M}|^2}_{\rm MRK} \simeq \frac{4g_s^4}{\mathbf{k}_{T3}^2 \mathbf{k}_{T4}^2} \tilde{P}_{qq}(z_1) \tilde{P}_{qq}(z_2) \frac{\overline{|\mathcal{A}_{PRA}|^2}}{z_1 z_2},$$

where $\overline{|\mathcal{A}_{PRA}|^2}$ is the **gauge-invariant** amplitude $Q_+(q_1) + \bar{Q}_-(q_2) \to \gamma^*(q)$ with **Reggeized** (**off-shell**) partons in the initial state.

In MRK regime

We can use Lipatov's Effective Field Theory of Reggeized gluons and Reggeized quarks to obtain $\mathcal{A}_{PRA}$.

LO MMRK factorization formula

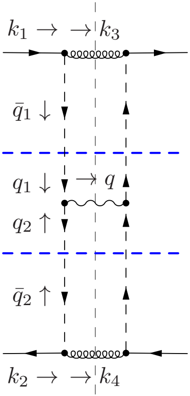

Modified MRK approximation: $z_{1,2}$ and $\mathbf{k}_{T3,4}^2$ – arbitrary

:

$$\overline{|\mathcal{M}|^2}_{\rm MMRK} \simeq \frac{4g_s^4}{\tilde{q}_1^2 \tilde{q}_2^2} P_{qq}(z_1) P_{qq}(z_2) \frac{\overline{|\mathcal{A}_{PRA}|^2}}{z_1 z_2},$$

where $\tilde{q}_{1,2}^2 = \mathbf{q}_{T1,2}^2/(1-z_{1,2})$, $P_{qq}(z)$ – DGLAP $q \to q$ splitting function. This factorization formula has correct **collinear** and **Multi-Regge** limits!

Factorization formula

Substituting the $\overline{|\mathcal{M}|^2}_{\rm MMRK}$ to the factorization formula of CPM and changing the variables we get:

$$d\sigma = \int\limits_0^1 \frac{dx_1}{x_1} \int \frac{d^2\mathbf{q}_{T1}}{\pi} \Phi_q^{(\rm tree-level)}(x_1, t_1, \mu_Y^2) \times \\ \times \int\limits_0^1 \frac{dx_2}{x_2} \int \frac{d^2\mathbf{q}_{T2}}{\pi} \Phi_{\bar{q}}^{(\rm tree-level)}(x_2, t_2, \mu_Y^2) \cdot d\hat{\sigma}_{\rm PRA},$$

where $x_1 = q_1^+/P_1+$, $x_2 = q_2^-/P_2^-$, $\Phi^{(\rm tree-level)}(x, t, \mu_Y^2)$ – "tree-level" **unintegrated PDFs**. The partonic cross-section in PRA is written as:

$$d\hat{\sigma}_{\rm PRA} = \frac{\overline{|\mathcal{A}_{PRA}|^2}}{2Sx_1x_2} \cdot (2\pi)^4 \delta\left(\frac{1}{2}\left(q_1^+ n_- + q_2^- n_+\right) + q_{T1} + q_{T2} - q(\gamma^*)\right) d\Phi(\gamma^*).$$

Note that **flux-factor** $2x_1x_2S$ for **off-shell** initial-state partons should be used.

Parton Reggeization Approach

Tree-level unintegrated PDFs:

$$\Phi_i^{(\text{tree-level})}(x,t,\mu_F,\mu_Y^2) = \frac{\alpha_s(\mu_R)}{2\pi}\frac{1}{t}\sum_{j=q,\bar{q},g}\int\limits_x^1 dz\, P_{ij}(z)F_j\left(\frac{x}{z},\mu_F^2\right)\theta\left(\Delta(t,\mu_Y^2)-z\right),$$

where $F_i(x,\mu_F^2) = xf_j(x,\mu_F^2)$. The θ-functions enforce the rapidity-ordering between particles in the final-state $y_3 > y_{\gamma^*} > y_4$, for our MMRK approximation for the squared amplitude and kinematics to be applicable. The KMRW cutoff function defines the region of applicability of MMRK:

$$\Delta(t,\mu) = \frac{\sqrt{\mu}}{\sqrt{\mu}+\sqrt{t}}.$$

Parton Reggeization Approach

Reggeized hadronic tensor

$$W_{\mu\nu}^{MMRK} = \sum_{k,l}\int_0^1 \frac{dx_1}{x_1}\int \frac{d^2\mathbf{q}_{T1}}{\pi}\Phi_k^{(\mathrm{tree-level})}(x_1,\mathbf{q}_{T1},\mu_Y)$$
$$\times \int_0^1 \frac{dx_2}{x_2}\int \frac{d^2\mathbf{q}_{T2}}{\pi}\Phi_l^{(\mathrm{tree-level})}(x_2,\mathbf{q}_{T2},\mu_Y)$$
$$\times (2\pi)^4\delta(q_1+q_2-q)\frac{w_{\mu\nu}^{MRK}}{2Sx_1x_2}$$

Reggeized partonic tensor, $Q(\tilde{q}_1)+\bar{Q}(\tilde{q}_2)\to\gamma^*(q)$

$$w_{\mu\nu}^{MRK} = \frac{(4\pi\alpha)}{4N_c}e_q^2\mathrm{tr}\left[\left(\frac{q_1^+}{2}\hat{n}_-\right)\Gamma_\mu^{(+-)}(q_1,q_2)\left(\frac{q_2^-}{2}\hat{n}_+\right)\Gamma_\nu^{(+-)}(q_1,q_2)\right]$$

Unintegrated PDFs with exact normalization

To resolve a divergence problem of $\Phi_i^{(\text{tree-level})}(x, t, \mu_Y^2)$

we follow the standard definition of the UPDF in BFKL formalism and require that:

$$\int_0^{\mu^2} dt\ \Phi_i(x, t, \mu^2) = F_i(x, \mu^2),$$

which is equivalent to:

$$\Phi_i(x, t, \mu^2) = \frac{d}{dt}\left[T_i(t, \mu^2, x) F_i(x, t)\right],$$

where $T_i(t, \mu^2, x)$ is usually referred to as *Sudakov formfactor*, satisfying the boundary conditions $T_i(t = 0, \mu^2, x) = 0$ and $T_i(t = \mu^2, \mu^2, x) = 1$.

We ask exact equivalence between last ones and following (*KMRW*) prescription:

$$\Phi_i(x, t, \mu_Y^2) = \frac{\alpha_s(t)}{2\pi} \frac{T_i(t, \mu^2, x)}{t} \sum_{j=q,\bar{q},g} \int_x^1 dz\ P_{ij}(z) F_j\left(\frac{x}{z}, t\right) \theta\left(\Delta(t, \mu_Y^2) - z\right),$$

Unintegrated PDFs with exact normalization

The solution for Sudakov formfactor

$$T_i(t,\mu^2,x) = \exp\left[-\int_t^{\mu^2} \frac{dt'}{t'} \frac{\alpha_s(t')}{2\pi} \left(\tau_i(t',\mu^2) + \Delta\tau_i(t',\mu^2,x)\right)\right]$$

with

$$\tau_i(t,\mu^2) = \sum_j \int_0^1 dz\; zP_{ji}(z)\theta(\Delta(t,\mu^2)-z),$$

$$\Delta\tau_i(t,\mu^2,x) = \sum_j \int_0^1 dz\; \theta(z-\Delta(t,\mu^2))\left[zP_{ji}(z) - \frac{F_j\left(\frac{x}{z},t\right)}{F_i(x,t)}P_{ij}(z)\theta(z-x)\right].$$

MMRK PDFs versus KMRW PDFs

The Sudakov formfactor without the $\Delta\tau_i$-term in the exponent is similar to the Sudakov formfactor of LO KMRW UPDF but with a numerically-important difference that in our MMRK approach, **the rapidity-ordering condition is imposed both on quarks and gluons, while in KMRW-approach it is imposed only on gluons.**

Comparison PRA with Collins-Soper-Sterman fromalism

Collins-Soper-Sterman formula with perturbative resummation of higher-order corrections enhanced by $\ln(Q^2/\mathbf{q}_T^2)$

$$\frac{d\sigma}{dQ^2 d\mathbf{q}_T^2 dy} = \frac{\alpha}{3\pi Q^2 Q_T^2} \sum_{j,a,b} \frac{(4\pi\alpha)e_j^2}{4N_c} \int d^2\mathbf{x}_T e^{i\mathbf{q}_T\mathbf{x}_T} \times$$

$$\times \quad \left[\int_{x_+}^{1} \frac{dz_+}{z_+} \tilde{f}_a \left(\frac{x_+}{z_+}, \frac{1}{\mathbf{x}_T^2} \right) C_{ja}(z_+, \alpha_s(1/\mathbf{x}_T^2)) \right]$$

$$\times \quad \left[\int_{x_-}^{1} \frac{dz_-}{z_-} \tilde{f}_a \left(\frac{x_-}{z_-}, \frac{1}{\mathbf{x}_T^2} \right) C_{ja}(z_-, \alpha_s(1/\mathbf{x}_T^2)) \right] \times S(\mathbf{x}_T^2, Q^2),$$

Comparison PRA with Collins-Soper-Sterman fromalism

Sudakov formfactor in the $\mathbf{x}_T$-space:

$$S(\mathbf{x}_T^2, Q^2) = \exp\left[- \int\limits_{1/\mathbf{x}_T^2}^{Q^2} \frac{dt'}{t'} \left(A(\alpha_s(t')) \ln \frac{Q^2}{t'} + B(\alpha_s(t')) \right) \right],$$

where functions A and B, corresponding respectively to the resummation of doubly ($\propto \ln^2(\mathbf{x}_T^2 Q^2)$) and single-logarithmic ($\propto \ln(\mathbf{x}_T^2 Q^2)$) corrections admit the following perturbative expansion:

$$\begin{aligned} A(\alpha_s) &= C_F \frac{\alpha_s}{\pi} + O(\alpha_s^2), \\ B(\alpha_s) &= 2C_F \left[-\frac{3}{4} + \ln \frac{C_1}{2C_2} + \gamma_E \right] \frac{\alpha_s}{\pi} + O(\alpha_s^2), \end{aligned}$$

Comparison PRA with Collins-Soper-Sterman fromalism

We should compare

$$\sqrt{S(\mathbf{x}_T^2, Q^2)} \quad \text{with Fourier-transform of } \frac{dT_q(\mathbf{q}_T^2, Q^2)}{d\mathbf{q}_T^2} \to \tilde{T}(\mathbf{x}_T^2, Q^2)$$

Taking into account, that for $t \ll Q^2$: $1 - \Delta(t, Q^2) \simeq \sqrt{t/Q^2}$, one obtains in this limit:

$$T_q(t, Q^2) \simeq \exp\left[-\frac{\alpha_s}{2\pi} C_F \left(\frac{1}{2} \ln^2 \frac{Q^2}{t} - \frac{3}{2} \ln \frac{Q^2}{t}\right)\right],$$

Here, up to NLL approximation

$$\Phi_q(x, t, Q^2) = \frac{d}{dt}\left[T_q(t, Q^2, x) F_q(x, t)\right] \approx F_q(x, t) \frac{dT(t, Q^2, x)}{dt}$$

It has

$$\tilde{T}(\mathbf{x}_T^2, Q^2) \approx \exp\left[-\frac{\alpha_s}{2\pi} C_F \left(\frac{1}{2} \ln^2(Q^2 \mathbf{x}_T^2) - \frac{3}{2} \ln(Q^2 \mathbf{x}_T^2)\right)\right]$$

The last result indeed coincides with the square-root of $S(\mathbf{x}_T^2, Q^2)$ in a scheme with $\ln C_1/(2C_2) = -\gamma_E$. So, our resummation scheme is consistent with perturbative part of CSS formalism up to NLL-approximation in the region $\mathbf{q}_T^2 \ll Q^2$, thanks to a particular small-t asymptotic of the KMRW cutoff function: $1 - \Delta(t, Q^2) \simeq \sqrt{t/Q^2}$.

Nonperturbative part of UPDFs

Analogously with KMRW

We define the UPDF for $t < t_0 = 1$ GeV as

$$t\Phi_i(x, t, \mu^2) = At^{1+\alpha}(t_1 - t),$$

where parameters A, t_1 and α are determined from the requirements of normalization of UPDF, it's continuity, smoothness in the point $t = t_0$ and positivity of α.

Intrinsic motion

The UPDF defined for all values of t as described above we call the *shower-part* of the UPDF. Physically it is determined by perturbative dynamics of QCD for $t > t_0$ and nonperturbative properties of QCD vacuum for $t < t_0$. To take into account non-perturbative intrinsic motion of partons inside hadron we convolute the shower part on UPDF with phenomenological intrinsic transverse-momentum distribution, which we take in the x-independent Gaussian from:

$$\Phi_i(x, \mathbf{q}_T^2, \mu^2) = \int \frac{d^2\mathbf{k}_T}{\pi\sigma_{Ti}^2} e^{-\frac{\mathbf{k}_T^2}{\sigma_{Ti}^2}} \Phi_i^{(\text{shower})}(x, (\mathbf{q}_T - \mathbf{k}_T)^2, \mu^2).$$

DY production at $\sqrt{S} \leq 200$ GeV

We have found $\sigma_T = 0.35$ GeV and $\chi^2/d.o.f. = 1.5$ with 323 data-points in analysis

TABLE I. Experimental data on transverse-momentum spectra of Drell-Yan lepton pairs used in the present study and corresponding values of K-factors. The ATLAS-2019 and CDF-1999 data are not included into the fit of σ_T.

Dataset	Observable	$\sqrt{S}$(GeV)	Q(GeV)	$\frac{\sigma(\text{data})}{\sigma(\text{theory})}$ [+/− scale-uncert.] (+/− exp. uncert.)
E-288 [3]	$q^0 d\sigma/d^3q$	19.4	4–5	1.54[+0.63/−0.40](±0.20)
			5–6	1.50[+0.70/−0.45](±0.18)
			6–7	1.43[+0.73/−0.46](±0.18)
			7–8	1.22[+0.70/−0.43](±0.25)
			8–9	1.03[+0.64/−0.04](±0.35)
		23.7	4–5	1.64[+0.56/−0.35](±0.22)
			5–6	1.46[+0.57/−0.36](±0.14)
			6–7	1.47[+0.64/−0.42](±0.17)
			7–8	1.47[+0.70/−0.44](±0.20)
			8–9	1.43[+0.71/−0.45](±0.29)
		27.4	5–6	1.57[+0.55/−0.33](±0.13)
			6–7	1.47[+0.57/−0.36](±0.07)
			7–8	1.44[+0.60/−0.38](±0.08)
			8–9	1.35[+0.60/−0.38](±0.10)
E-605 [5]	$q^0 d\sigma/d^3q$	38.8	7–8	1.50[+0.55/−0.31](±0.18)
			8–9	1.42[+0.56/−0.33](±0.10)
			10.5–11.5	1.33[+0.60/−0.38](±0.11)
			11.5–13.5	1.40[+0.67/−0.40](±0.11)
			13.5–18	1.14[+0.60/−0.36](±0.17)
R-209 [4]	$d\sigma/d\mathbf{q}_T^2$	62	5–8	1.63[+0.40/−0.18](±0.29)
PHENIX [2]	$q^0 d\sigma/d^3q$	200	4.8–8.2	1.50[+0.17/−0.10](±0.44)
CDF-1999 [6]	$d\sigma/d\|\mathbf{q}_T\|$	1800	66–116	2.07[+0.23/−0.12](±0.11)
ATLAS-2019 [1]	$d\sigma/d\|\mathbf{q}_T\|$	13000	66–116	1.71[+0.07/−0.06](±0.04)

DY production at $\sqrt{S} \leq 200$ GeV

We have found $\sigma_T = 0.35$ GeV and $\chi^2/d.o.f. = 1.5$ with 323 data-points in analysis

TABLE I. Experimental data on transverse-momentum spectra of Drell-Yan lepton pairs used in the present study and corresponding values of K-factors. The ATLAS-2019 and CDF-1999 data are not included into the fit of σ_T.

Dataset	Observable	$\sqrt{S}$(GeV)	Q(GeV)	$\frac{\sigma(\text{data})}{\sigma(\text{theory})}$ [+/− scale-uncert.] (+/− exp. uncert.)
E-288 [3]	$q^0 d\sigma/d^3q$	19.4	4–5	1.54[+0.63/−0.40](±0.20)
			5–6	1.50[+0.70/−0.45](±0.18)
			6–7	1.43[+0.73/−0.46](±0.18)
			7–8	1.22[+0.70/−0.43](±0.25)
			8–9	1.03[+0.64/−0.04](±0.35)
		23.7	4–5	1.64[+0.56/−0.35](±0.22)
			5–6	1.46[+0.57/−0.36](±0.14)
			6–7	1.47[+0.64/−0.42](±0.17)
			7–8	1.47[+0.70/−0.44](±0.20)
			8–9	1.43[+0.71/−0.45](±0.29)
		27.4	5–6	1.57[+0.55/−0.33](±0.13)
			6–7	1.47[+0.57/−0.36](±0.07)
			7–8	1.44[+0.60/−0.38](±0.08)
			8–9	1.35[+0.60/−0.38](±0.10)
E-605 [5]	$q^0 d\sigma/d^3q$	38.8	7–8	1.50[+0.55/−0.31](±0.18)
			8–9	1.42[+0.56/−0.33](±0.10)
			10.5–11.5	1.33[+0.60/−0.38](±0.11)
			11.5–13.5	1.40[+0.67/−0.40](±0.11)
			13.5–18	1.14[+0.60/−0.36](±0.17)
R-209 [4]	$d\sigma/d\mathbf{q}_T^2$	62	5–8	1.63[+0.40/−0.18](±0.29)
PHENIX [2]	$q^0 d\sigma/d^3q$	200	4.8–8.2	1.50[+0.17/−0.10](±0.44)
CDF-1999 [6]	$d\sigma/d\|\mathbf{q}_T\|$	1800	66–116	2.07[+0.23/−0.12](±0.11)
ATLAS-2019 [1]	$d\sigma/d\|\mathbf{q}_T\|$	13000	66–116	1.71[+0.07/−0.06](±0.04)

DY production at $\sqrt{S} \leq 200$ GeV

Description of normalized $d\sigma/d\mathbf{q}_T^2/\sigma$-distributions for $\sqrt{S} \leq 200$ GeV with $\sigma_T^{(\text{best fit})} = 0.35$ GeV

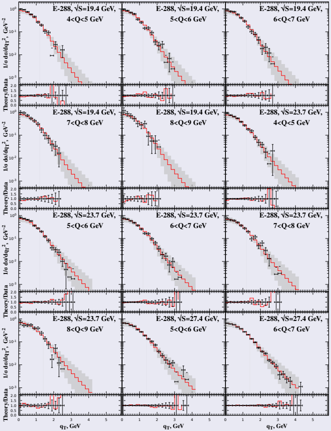

DY production at $\sqrt{S} \leq 200$ GeV

Description of normalized $d\sigma/d\mathbf{q}_T^2/\sigma$-distributions for $\sqrt{S} \leq 200$ GeV with $\sigma_T^{(\text{best fit})} = 0.35$ GeV

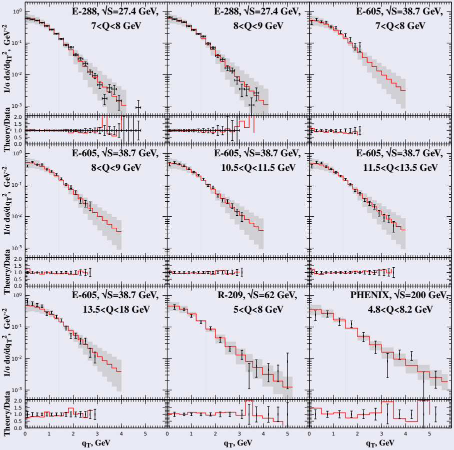

DY production at $\sqrt{S} = 1.96$ TeV

The normalized transverse-momentum spectrum of Drell-Yan lepton pairs measured by the CDF collaboration compared to LO PRA predictions made with LO (blue histogram) and NLO (red histogram) UPDFs. The uncertainty band is shown only for the LO prediction.

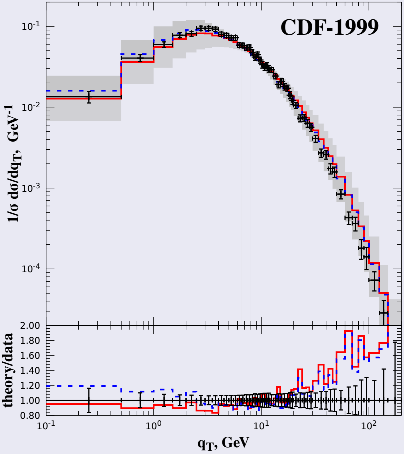

DY production at $\sqrt{S} = 13$ TeV

The normalized transverse-momentum spectrum of Drell-Yan lepton pairs measured by the ATLAS collaboration compared to LO PRA predictions made with LO (blue histogram) and NLO (red histogram) UPDFs. Left panel – $|\mathbf{q}_T| < 100$ GeV, right panel – $|\mathbf{q}_T| > 100$ GeV. The uncertainty band is shown only for the LO prediction.

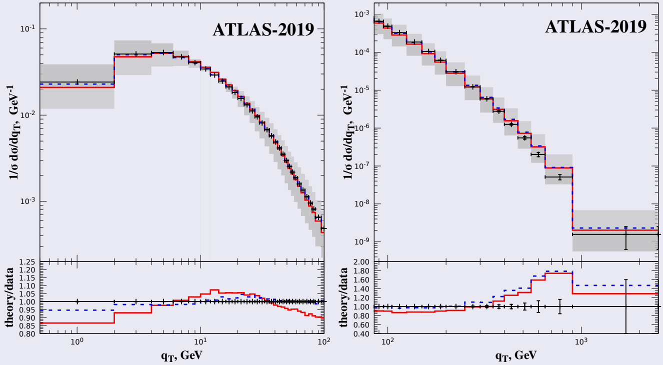

Angular coefficients

The angular distribution of leptons in the rest-frame of the lepton-pair

$$\frac{d\sigma}{dQ d\mathbf{q}_T^2 dy d\Omega_l} = \frac{3}{16\pi} \frac{d\sigma}{dQ d\mathbf{q}_T^2 dy} \Big\{ (1+\cos^2\theta_l) + \frac{A_0}{2}(1-3\cos^2\theta_l)$$
$$+ \quad A_1 \sin 2\theta_l \cos\phi_l + \frac{A_2}{2}\sin^2\theta_l \sin 2\phi_l + A_3 \sin\theta_l \cos\phi_l + A_4 \cos\theta_l$$
$$+ \quad A_5 \sin^2\theta_l \sin 2\phi_l + A_6 \sin 2\theta_l \sin\phi_l + A_7 \sin\theta_l \sin\phi_l \Big\},$$

$$\mu = \frac{2A_1}{2+A_0}, \quad \nu = \frac{2A_2}{2+A_0}, \quad \lambda = \frac{2-3A_0}{2+A_0}$$

Angular coefficients

Comparison with NuSea Collaboration data, $\sqrt{S} = 39$ GeV. Figures are from [M. Nefedov, N. Nikolaev, and V. Saleev, Phys. Rev. D 87, 014022 (2013).]

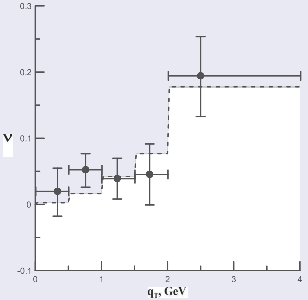

FIG. 8. Angular coefficient ν as a function of q_T. The histogram corresponds to LO calculation in PRA with KMR [34] unintegrated PDFs. The data are from the NuSea Collaboration [2].

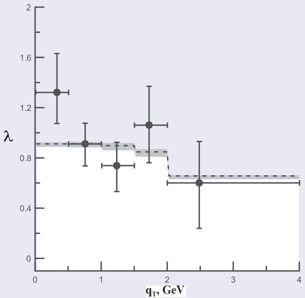

FIG. 9. Angular coefficient λ as a function of q_T. The histogram corresponds to LO calculation in PRA with KMR [34] unintegrated PDFs. The data are from the NuSea Collaboration [2].

Angular coefficients

Comparison of angular coefficients nonzero in the LO of PRA with corresponding experimental data obtained by ATLAS Collaboration. Left panel: blue histogram and points – A_0, red histogram and points – A_2. Right panel: blue histogram and points – A_1, red histogram and points – A_3, green histogram and points – A_4.

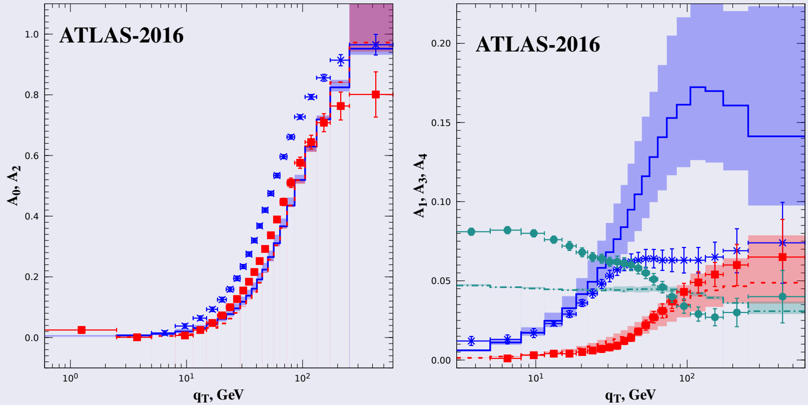

Conclusions

- We have introduced a new model to obtain UPDF from LO and NLO collinear PDFs and to define it's non-perturbative ambiguity.
- This UPDF, together with QCD and QED gauge-invariant matrix elements already in the LO in α_s provide an excellent description of shapes of transverse-momentum distributions of DY lepton-pairs in pp and $p\bar{p}$-collisions at low and high collision energies, in the region $Q_T/\sqrt{S} \ll 1$.
- Qualitative description of transverse-momentum dependence of angular coefficients of lepton distribution in the rest frame of the lepton pair is also achieved for $Q \simeq M_Z$.
- To describe the normalization of $|\mathbf{q}_T|$-distribution and extend the formalism to higher values of transverse momenta it is necessary to go beyond LO in α_s for the coefficient function in our approach. The formalism of NLO calculations is currently under development, **see talk by Maxim Nefedov, 09.12.2020**:
  A. van Hameren, arXiv:1710.07609. 931 [70]]; E. Blanco, A. van Hameren, P. Kotko, and K. Kutak, 932 arXiv:2008.07916. 933; M. Nefedov and V. Saleev, Mod. Phys. Lett. A 32, 1750207 934 (2017). 935; M. A. Nefedov, Nucl. Phys. B946, 114715 (2019).